Energy Conversion and Management 76 (2013) 665–673

Contents lists available at ScienceDirect

Energy Conversion and Management

journal homepage: www.elsevier.com/locate/enconman

Comprehensive analysis of pipeline transportation systems for CO_2 sequestration. Thermodynamics and safety problems

Andrzej Witkowski *, Andrzej Rusin, Mirosław Majkut, Sebastian Rulik, Katarzyna Stolecka

Institute of Power Engineering and Turbomachinery, Konarskiego 18, 44-100 Gliwice, Poland

ARTICLE INFO

Article history:
Received 9 November 2012
Accepted 29 July 2013

Keywords:
Compression systems
Pipeline transport
Hazard identifications

ABSTRACT

The aim of this paper is to analyze CO_2 compression and transportation processes with safety issues for post-combustion CO_2 capture applications for basic technological concepts of a 900 MW pulverized coal-fired power plant. Four various types of compressors including a conventional multistage centrifugal compressor, an integrally geared centrifugal compressor, a supersonic shock wave compressor, and pump machines were used. This study emphasizes that total compression power is a strong function of the thermodynamic process and is not only determined by the compressor efficiency. The compressor increases the CO_2 pressure from normal pressure to critical pressure and the boosting pump continues to increase the pressure to the required pressure for the pipeline inlet. Another problem analyzed in this study is the transport of CO_2 by pipeline from the compressor outlet site to the disposal site under heat transfer conditions. Simulations were made to determine maximum safe pipeline distance to subsequent booster stations depending on inlet pressure, environmental temperature, the thermal insulation thickness and the ground level heat transfer conditions. From the point of view of environmental protection, the most important problem is to identify the hazards which indirectly affect CO_2 transportation in a strict and reliable manner. This identification is essential for effective hazard management. A failure of pipelines is usually caused by corrosion, material defects, ground movement or third party interference. After the rupture of the pipeline transporting liquid CO_2, a large pressure drop will occur. The pressure will continue to fall until the liquid becomes a mixture of saturated vapour/liquid. In the vicinity of the rupture, liquid CO_2 will escape and immediately vaporize and expand. In the paper the discharge and atmospheric dispersion of CO_2 are discussed.

1. Introduction

CO_2 compression and transportation issues have a long tradition in modern industrial processes. They are gaining importance in the current worldwide discussion of the global climate change. Anthropogenic carbon dioxide emissions arise mainly from combustion of fossil fuels [1] and biomass in power generation, air-blown gasification [2], industrial processes such as cement manufacture [3], natural gas processing, hydrogen production and petroleum refining [4], building and transport sectors. CO_2 is also emitted from non-combustion sources in certain industries. CO_2 capture and storage (CCS) solutions present opportunities to reduce the problem. However, it is the modern pulverized coal-fired power plants that are most responsible for CO_2 emissions. The CO_2 capture and storage chain is subdivided into four systems: the system of capture and compression, the transport system, the injection system and the storage system. The main objective of this paper is to analyze the CO_2 compression and transportation systems. The first part presents an analysis of the processes related to the compression of CO_2 captured from flue gases of the concept 900 MW power plant intended for the firing of pulverized hard coal [5] to the pressure value at the transporting pipeline inlet using as little energy as possible. Among several approaches to CO_2 transport, pipeline transportation is the most economical solution to transport large amounts of CO_2 for a long distance [6–9]. Normally, it is recommended that the pipeline should be operated at high pressure, higher than the critical pressure to increase the transport capability and reduce the capital cost of the pipeline system [9]. Pressure losses and sufficient pipeline distances taken into account require compressor discharge pressure in the range of 130–200 bar [10–14]. CO_2 compression differs from most fluid compression tasks due to high molecular weight, highly compressible behaviour and the presence of the critical point. At the critical point, the difference between the fluid liquid and gaseous phases disappears. During the compression process, the reduction in CO_2 volume is tremendous. The consequence is the large impeller of the first and the very small impeller of the last stage. This results in high efficiency of the first stage and substantially lower values of efficiency of the subsequent stages. Existing CO_2 compressors are

* Corresponding author. Tel.: [redacted]
E-mail address: [redacted]@polsl.pl (A. Witkowski).

0196-8904/$ - see front matter © 2013 Elsevier Ltd. All rights reserved.
http://dx.doi.org/10.1016/j.enconman.2013.07.087

Nomenclature

k	heat exchange coefficient (W/(m^2 K))
L	distance along pipeline (m)
$\dot{m}$	transport flow rate (kg/s)
N_c	compression power (kW)
N_{ci}	compression input power (kW)
N_p	pumping power (kW)
N_s	shaft power (kW)
P	CO_2 pressure (bar)
Q	heat of compression (kW)
$Q_{r90°}$	total heat recoverable to 90 °C (kW)
r_1	internal radius of pipe (m)
r_2	external radius of pipe (m)
r_z	external wall radius of the thermal insulation layer (m)
t_{amb}	ambient temperature (°C)
t_i	CO_2 temperature on the pipeline inlet (°C)
t_{in}	intercooling CO_2 temperature (°C)
z	distance between the ground surface and the pipe centre (m)

Greek symbols

α_{ag}	convection heat transfer coefficient between air and the ground surface (W/(m^2 K))
η	efficiency
λ_{pw}	heat conductivity of the pipe wall (W/m^2)
λ_{soil}	heat conductivity of the soil (W/m^2)
λ_{ti}	heat conductivity of the thermal insulation (W/m^2)
Π	pressure ratio
ρ	CO_2 density (kg/m^3)

Subscripts

1, 2, 3	stations in the compressor stage
amb	ambient conditions
p	polytrophic process, pump
s	shaft
st	stage
t	total

expensive because the overall pressure ratio is very high (100:1) and, in part, because they require a stainless steel construction to accommodate CO_2 in the presence of water vapour. By far the most significant impact on cost is the aerodynamic design practice that limits the design pressure ratio per stage for heavier gases such as CO_2. Thanks to it, CO_2 compressors are responsible for a large portion of the enormous capital and operating cost penalties expected with any carbon capture and sequestration system (CCS). The CO_2 compressor power required for a pulverized coal-fired power plant with amine-based capture systems amounts to approximately 8–12% of the plant rating [11,12], depending on operating conditions, and it cannot be fully optimized without considering the significant amount of heat compression. To optimize heat integration [12,13], compression systems must be integrated with both the power unit and the CO_2 capture installations. In view of the fact that the selection and design of an efficient CO_2 compression technology is dependent on the applied carbon separation method [1], the present work is motivated by the need to gain a better understanding of the possibilities and limitations of the CO_2 compression process for post-combustion CO_2 capture applications. This paper contains a technical overview of seven types of compression technologies, all of which are applicable to CO_2 applications. In the last decade the understanding of CCS technologies has improved greatly [7–9,14,15]. However, there are still no quantitative conclusions concerning CO_2 properties in transport under variable ambient temperatures or the influence of thermal insulation obtained from the calculation of the heat exchange along the pipeline between the CO_2 in the pipe and the surroundings. The simulations made in this work determine the maximum safe distances of the pipeline to subsequent booster stations as a function of ambient temperature and thickness of the thermal insulation layer. The most important question is whether the thermal insulation layer on the external surfaces of the pipeline is necessary in the Polish climate to extend the maximum safe transport distance. There are also still significant gaps in the knowledge of integrated compression and transport processes taking safety issues into consideration. Many studies of carbon capture processes have been undertaken but few of them refer to compression and transport models to determine an integrated CCS process. Therefore, this paper focuses on compression as well as transportation processes with particular stress on the safety risk related to the transport of CO_2.

2. Thermodynamic evaluation of CO_2 compression strategies

2.1. Boundary conditions

Specifically, this study aims at a clear characterization of the CO_2 compression process for basic technological concepts of a capture-ready 900 MW hard coal-fired power plant described in [5]. The basic parameters of such a plant are listed in the Table 1.

In a typical post-combustion capture process based on chemical absorption, CO_2 is separated from the exhaust gas stream of the power plant at close-to-ambient conditions (t_1 = 28 °C, p_1 = 1.51 bar). The compressor power was calculated for the following remaining conditions: discharge pressure 153 bar, CO_2 mass flow rate 156.4 kg/s, cooling water temperature 19 °C, interstage cooling gas temperature, realistic 38 °C, pressure loss in the coolers 1–3% (Δp_{max} < 0.344 bar). These thermodynamic properties were used throughout the thermodynamic analysis to compare alternative options to the power required for the conventional compression process.

2.2. Thermodynamic analysis

The process simulation Aspen Plus software package [16] was used to predict thermodynamic properties of the CO_2 stream at required conditions and quantify the performance of each compression chain option accordingly. Within the Aspen environment, the Benedict, Web, and Rubin with extension by Starling (BWRS) and Redlich and Kwong augmented by Soave (LKP) equation of state for real gases within the relevant ranges of pressure and temperature for the process compressor were used. The results for carbon dioxide [17] are as follows: BWRS best agreement for p_{max} < 50 bar

Table 1
Basic parameters of the power plant.

Parameter	Unit	Value
Electric power – gross	MW	900
net power	MW	832.56
Electricity generation efficiency (gross)	%	49.06
Electricity generation efficiency (net)	%	45.38
CO_2 mass flow in flue gases	kg/s	176.43
CO_2 capture degree	%	~ 89

(>99.8%), LKP best agreement for 50–250 bar (>98%). The Beggs and Brill method [18], taking account of the general mechanical energy balance and average in situ density to calculate the pressure gradient, was used.

2.3. Compression technology options

Various types of compressors, including conventional in-line centrifugal 16 stage compression with six sections and five intercooling steps and integrally geared centrifugal machines, feature a multi-shaft arrangement with different speeds driven by a speed increasing gear and a constant speed electric motor. The first constitutes the baseline, against which all other alternatives are compared. The aerodynamic advantage of the second compressor results from the very high pressure ratio of 1.7–2:1, the wide range of flow coefficients and the intensive intercooling between all individual stages. Optimized shaft speeds, modern impellers and external cooling after each stage guarantee the highest efficiency. At these stage pressure ratios, eight stages of the integral-gear compressor are typically required to reach an overall pressure ratio of 100:1 (Figs. 1 and 2). During the compression process, the CO_2 volume reduction is tremendous. The consequence is the large impeller of the first and the very small impeller of the last stage. As a result, the polytrophic efficiency of this compressor was taken as 84% for the first stage and reduced linearly for each subsequent stage to 70% for the last stage. The CO_2 stream is brought to final pressure through compression sections intercooled to 38 °C.

The heat of the compression discharge temperature associated with these stage pressure ratios is approximately 90 °C, which, as the temperature of inflow to the next stage, is too high to achieve good efficiency but still lacks the thermal driving force for a cost-effective heat exchanger selection. This heat is also of insufficient quality to be of practical use elsewhere in the process. One possible option is to reject the 7th intercooler heat exchanger (Fig. 2). Since CO_2 is a highly corrosive medium, the water content must be reduced to less than 60% of the saturation state. The use of stainless steel for components in contact with wet CO_2 eliminates the problem.

An original and very promising concept – a high-efficiency gas compressor – has been developed lately [10,13,15]. It employs the same shock compression technology which is used in supersonic aircraft inlet systems. This compression is uniquely suited to the compression of large volumes of CO_2 and promises to significantly reduce gas compression auxiliary loads in CCS systems with high efficiency (85–86%). In addition to the obvious economic advantages and in view of the fact that the direct result of this compressor makes it possible to achieve single stage compression ratios of 10–12:1, the stage discharge temperature is about 285 °C (Fig. 3). The available heat may potentially be used to regenerate amine solutions or pre-heat the boiler feed-water. The final issue under analysis was the pumping of carbon dioxide in a liquid state at a low temperature (Figs. 4 and 5). The underlying premise of the liquefaction approach is that liquid pumps require significantly less power to raise pressure and are considerably less expensive than gas compressors.

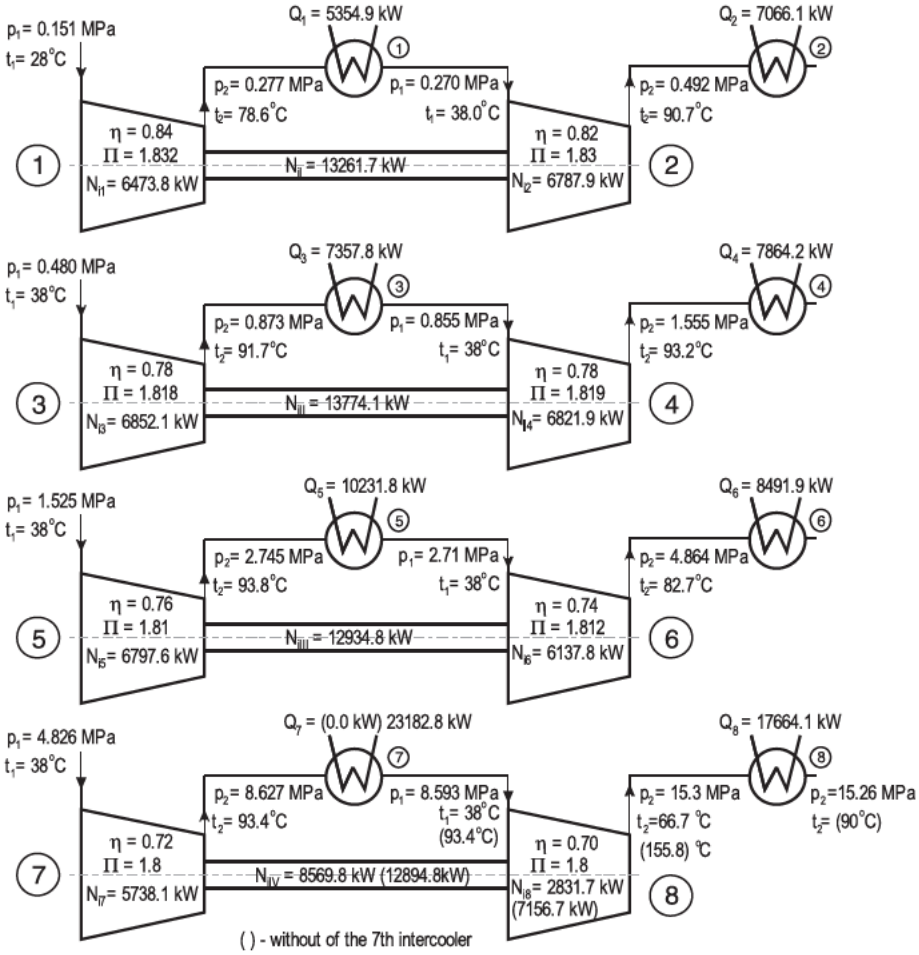

Fig. 1. Schematic illustration of the eight stage integrally geared compressor.

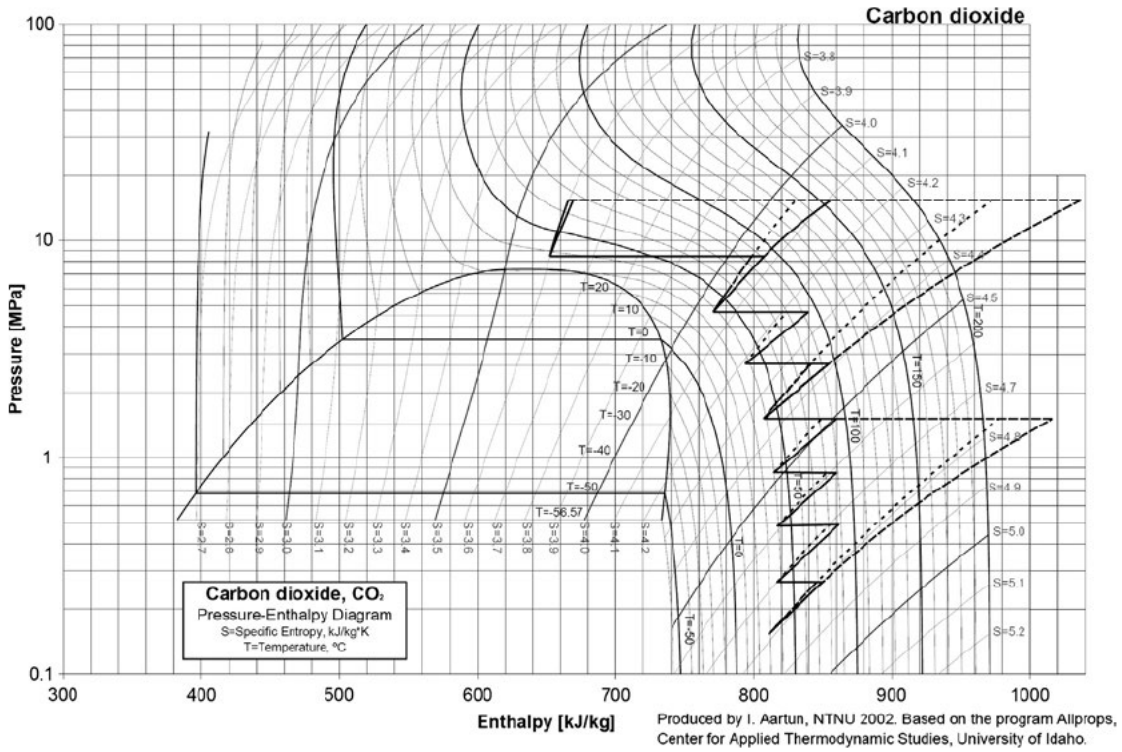

Fig. 2. Comparison of the thermodynamic path of CO_2 compression strategies of the eight stage integrally geared compressor and of Ramgen's supersonic shock wave two stage compressor.

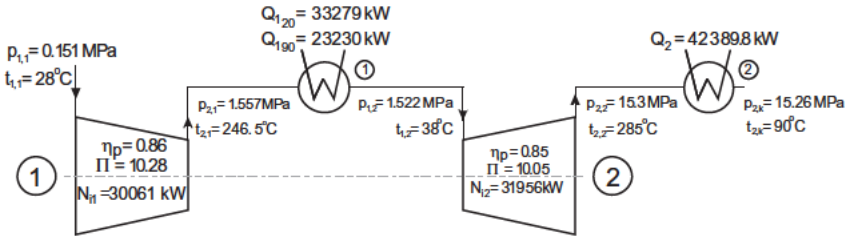

Fig. 3. Schematic illustration of the supersonic two stage compressor intercooled to 38 °C.

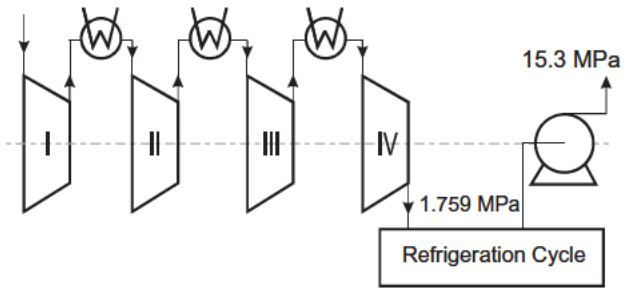

Fig. 4. Schematic illustration of the compression and refrigeration pumping cycle.

2.4. Summary of compression options

Table 2 summarizes the compression options considered in the analysis and the power requirement for each thermodynamic process. Option C_2 (Table 2) shows that integrally geared centrifugal compressors with intercoolers between each stage result in 16% power savings above baseline case C1.

The most important step of CO_2 compression integration into the power plant is the intercooler heat recovery. Therefore, a certain temperature level must be reached in the heat exchangers to generate useful heat by the rejection of the 7th intercooler in the eighth stage of the integrally geared compressor (option C3) [13]. This disadvantage of having a higher compression temperature after the last stage by leaving the ideal process of isothermal compression can be compensated for by the advantage of 33.4% heat recovery and 8.42% reduction in power. The benefits of the advanced shock wave compression technology (option SW) when applied to a high mole weight gas such as CO_2 are competitive efficiencies, a very high pressure ratio, a reduction in weight and in the capital cost, compared to comparable traditional equipment. An additional benefit of the two stage compressor is that the heat of compression discharge temperature is high enough to be useful in the surrounding processes (Table 3). Other options use centrifugal compression followed by liquefaction and pumping (options CP1–CP3). These options are summarized in Table 4. The results

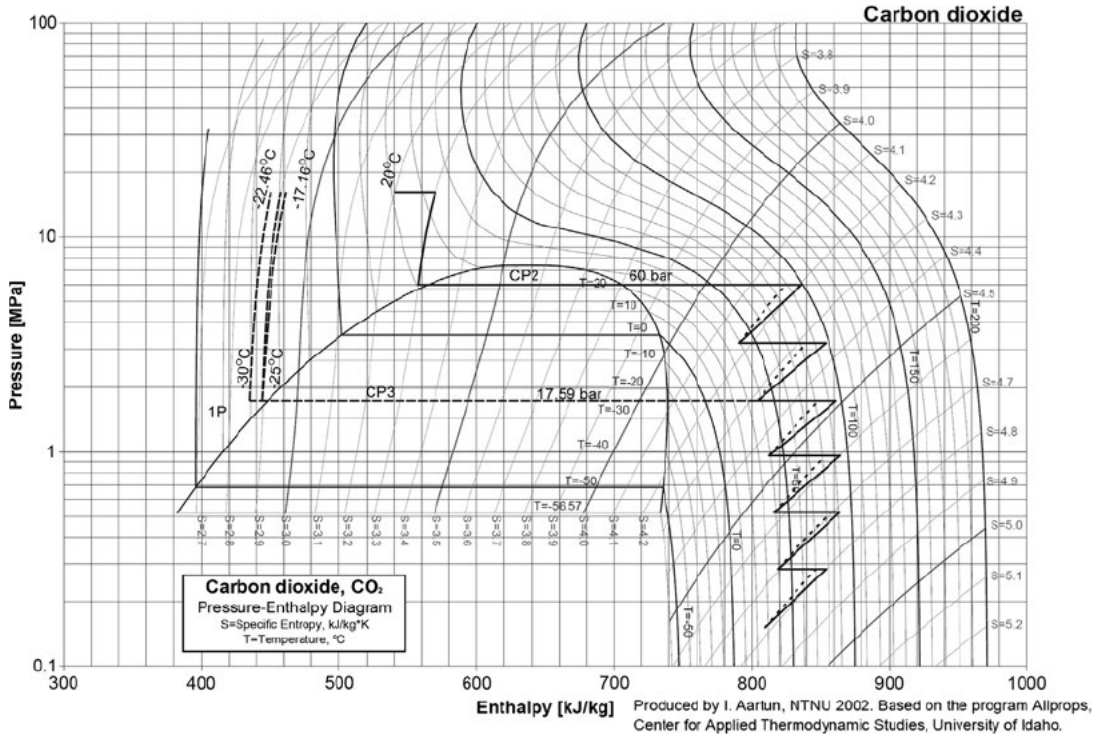

Fig. 5. Thermodynamic path of CO_2 compression and the analyzed pumping strategies.

Table 2
Comparison of compression technology options.

Option	Compression technology	Process definition	Power requirements N_s (kW)	% Difference from option C1
C1	Conventional centrifugal 16 stage four section compressor	P_1 = 1.515 bar, P_2 = 153 bar t_1 = 28 °C, t_{in} = 38 °C η_p = 85–70%	57 787.42	0.0
C2	Eight stage centrifugal geared compressor with 7 intercoolers	P_1 = 1.515 bar, P_2 = 153 bar t_1 = 28 °C, t_{in} = 38 °C η_p = 84–70%	48 540.40	16
C3	Eight stage centrifugal geared compressor without of the 7th intercooler	P_1 = 1.515 bar, P_2 = 153 bar t_1 = 28 °C, t_{in} = 38 °C η_p = 84–70% Heat recoverable to 90 °C	52 919.3 17 664.10	8.42 33.4

Table 3
Comparison of energy balance of integrally geared compressors and shock wave compressors.

	Integrally geared eight stage compressor t_{in} = 38 °C Option C3	Shock wave compressor (SW) t_{in} = 38 °C Option SW
Total inner output $N_{\Sigma i}$ (kW)	52 919.30	62 017
Total heat of compression $Q_{\Sigma r}$ (kW)	69 549.54	75 668.8
Total heat recoverable to 90 °C $Q_{r90°C}$ (kW)	17 664.10	65 619.8

for cases CP1 and CP2 show that the power requirement can be reduced by up to 14.6% at the compressor outlet pressure of 80 bar and by up to 20.4% at the subcritical pressure of 60 bar. This minimum liquefaction pressure is dictated by the cooling medium temperature if water at ambient conditions is used. In order to evaluate the potential of liquefying CO_2 at a pressure below the minimum of 60 bar, CO_2 is cooled to a temperature below ambient during liquefaction at cryogenic pressure. As it can be seen in Fig. 5, the stream of CO_2 is brought to liquefaction pressure 17.59 bar through four compression sections intercooled to 38 °C with water. The final temperature of CO_2 directly after pumping is very low at 25 °C. The combination of the integrated gear compression with the liquefaction process resulted in the greatest energy savings at a 45.83% reduction in compression power compared to the conventional process. However, the liquefaction of carbon dioxide requires large amounts of refrigeration energy.

3. Pipeline CO_2 transport modelling for the case study

3.1. General remarks

Pipeline transmission of CO_2 over longer distances is most efficient when CO_2 is in the dense phase i.e. under the liquid or supercritical regime. In the following discussion, we will use the same

Table 4
Summary of compression and pumping power reduction.

Option	Compression technology	Process definition	Power requirements	% Difference from option C1
CP1	Six stage integrally geared compressor with five interstage coolers	P_1 = 1.515 bar, P_2 = 80 bar t_1 = 28 °C, t_{in} = 38 °C η_p = 0.84–0.72 π_{st} = 1.937	N_c = 46 750 kW	
	Pumping with supercritical liquefaction	P_1 = 80 bar , t_1 = 31 °C η_p = 0.8	N_p = 2 582.9 kW $N_c + N_p$ = 49 332.9 kW	14.6
CP2	Six stage integrally geared compressor with five interstage coolers	P_1 = 1.515 bar, P_2 = 60 bar t_1 = 28 °C, t_{in} = 38 °C η_p = 0.84–0.73 π_{st} = 1.846	N_c = 43 718.2 kW	
	Pumping with subcritical liquefaction	P_1 = 60 bar t_1 = 2°°C η_p = 0.8	N_p = 2 257.6 kW $N_c + N_p$ = 45 975.8 kW	20.4
CP3	Four stage integrally geared compressor with three interstage coolers	P_1 = 1.515 bar, P_2 = 17.59 bar t_1 = 28 °C, t_{in} = 38 °C η_p = 0.84–0.76 π_{st} = 1.846	N_c = 28 910.0 kW	
	Refrigerated pumping	P_1 = 17.59 bar, P_2 = 153 bar t_1 = – 25 °C ρ_2 = 1 015.89 kg/m^3	N_p = 2392.7 kW $N_T = N_c + N_p$ N_T = 31 302.7 kW	45.8

power station data as mentioned in Section 2. To agree with McCoy [7], a minimum injection pressure of 9 MPa for enhanced oil recovery (EOR) was assumed as the basic assumption for this pipeline model. Therefore, if CO_2 pressure dropped below 9 MPa, a boosting station would be installed to restore the pressure value to 153 MPa.

3.2. Energy balance with surroundings

In the process of designing a new CO_2 transportation pipeline, the most important problem is to find the maximum safe transport distance. For longer transport distances, a boosting pump station should be installed, to restore the pressure value to 153 bar. At a given inlet pressure, the safe transportation distance depends strongly on ambient temperature. An increase in ambient temperature reduces CO_2 density and increases the velocity along the pipeline, which, in turn, increases the pressure drop and leads to building up choking conditions. A bigger pressure drop means higher operating costs and possibly the need to introduce recompression stations. Hence, any optimization of CO_2 transport via a pipeline must take account of the impact of ambient temperature because of the heat exchange between CO_2 in the pipe and the surroundings along the pipeline. When designing the pipeline, the extreme case with the highest environmental temperature should be considered to ensure that the pipeline can work well all through the year. For the purposes of the study, the maximum value of ambient temperature, which in Poland may be as high as 30°°C, was assumed. This would significantly shorten the maximum distance at a given inlet pressure. In order to compare safe distances of CO_2 transportation at the highest and lower ambient temperatures, calculations were made also for 20 °C, 15 °C, and 0 °C.

Due to reasons of environmental safety, pipelines are often buried at a depth of 1.2–1.5 m, which ensures more stable temperatures than on the surface. The cross-section of a buried and insulated pipeline is shown in Fig. 6. A two dimensional heat formula can be used to calculate the heat exchange coefficient between the ground conduction and the CO_2 in the pipeline giving [19]:

$$k = \frac{1}{\frac{r_1}{\lambda_{pw}} \ln\frac{r_2}{r_1} + \frac{r_1}{\lambda_{ti}} \ln\frac{r_z}{r_2} + \frac{r_1}{\lambda_{soil}} \ln\frac{2z}{r_z} + \frac{r_1}{z}\frac{1}{\alpha_{ag}}}$$

where heat conductivity of the pipe wall material is λ_{pw} = 25 W/(mK), and that of the heat insulation layer material is λ_{ti} = 0.058 - W/(mK). The thermal conductivity of the soil is assumed to be λ_{soil} = 1.21 W/(mK), and the distance between the ground surface and the pipe centre is 1.225 m. The air convection heat transfer coefficient is 5 W/(m^2°K). According to [7,8], the thermal resistance of the convective thermal transfer between the CO_2 and the inner pipe wall is much smaller than that of the pipe wall and the heat insulation layer, so it is assumed that the temperature of the inner pipe wall is equal to the temperature of CO_2 at the same cross section. The value of the heat transfer coefficient k between the ground and CO_2 calculated from the equation for pipelines with 0.05 m and 0.03 m heat insulation will be 0.7387 and 0.912 W/(m^2°K), respectively, and for a pipeline without insulation the coefficient will be 2.11 W/(m^2°K). Resistance to heat transfer from the tubing and casing is ignored, as the conductivity of the steel used in the tubing and casing is at least an order of magnitude larger than any other conductivity in the system.

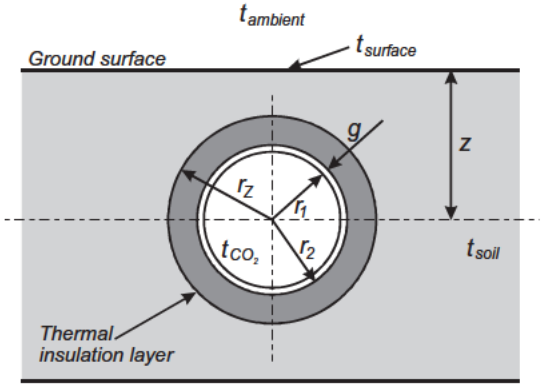

Fig. 6. Cross section of a buried and insulated pipeline.

3.3. Influence of ambient temperature and the thermal insulation layer on thermodynamic properties of the CO_2 flow in the pipeline

The pressure drop along the pipeline is dependent on the flow velocity, ambient temperature, the thermal insulation layer, as well as on geometric characteristics of the pipeline such as length and elevation changes. In order to understand the impact of the thermal insulation layer, the pipeline operational parameters were

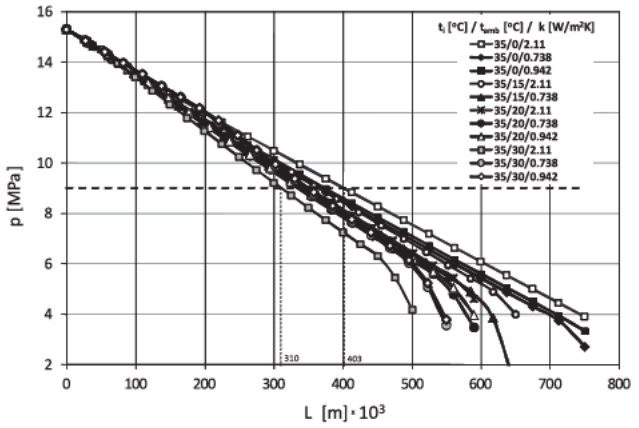

Fig. 7. Comparison of the pressure drop along a pipeline with and without thermal insulation at different ambient temperatures.

calculated with and without the insulation layer for different thicknesses and ambient temperatures.

Fig. 7 shows the pressure drop along a 0.05 m pipeline (k = 0.738 W/m^2°K), a 0.03 m pipeline (k = 0.942 W/m^2°K) and a pipeline without insulation (k = 2.11 W/m^2/K) at different ambient temperatures (0°°C, 15°°C, 20°°C and 30°°C). In the simulation, the inlet conditions for CO_2 are fixed. Carbon dioxide is transported to the injection site in a straight line over flat ground. It can be seen that an increase in ambient temperature reduces CO_2 density and increases the velocity along the pipeline, which, in turn, increases the pressure drop and leads to building up choking conditions at a certain distance. Fig. 8 shows more clearly the maximum safe transport distance of the CO_2 pipeline at different ambient temperatures, with and without a thermal insulation layer. It can be seen that if the inlet temperature is kept constant, the pressure drop increases when ambient temperature gets higher since velocity increases. At lower ambient temperatures, the pressure drop in a pipeline without thermal insulation is lower than in an insulated pipeline. It can be seen that the maximum difference in the maximum safe transport distance up to assumed pressure drops to below 9 MPa (about 32.8 km) for the two cases with and without insulation exists between CO_2 transmission at an ambient temperature of 0°°C. However, this difference is reduced to nearly none as ambient temperature rises to about 27°°C. The safe transport distance is longer for the case with insulation only at an ambient temperature higher than 27 °C. This verifies our estimation that a pipeline without thermal insulation is preferable for pipeline

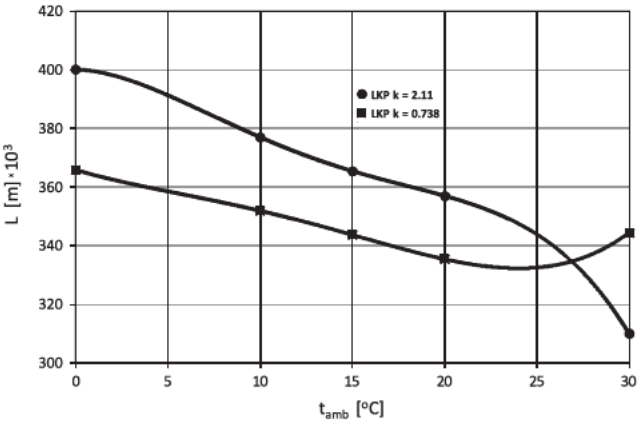

Fig. 8. Maximum pipeline distance, with and without an insulation layer, to subsequent booster stations at different ambient temperatures.

transport in the Polish climate. However, pipelines without thermal insulation should be designed for a shorter safe distance of up to 310 km (Fig. 8).

4. Aspects of safety related to CO_2 transport

4.1. The risk related to CO_2 transport

The assessment of risk related to the carbon dioxide capture and storage technology has to be carried out for each stage of the process, i.e. for the capture, transport, injection and storage of CO_2.

The following might occur at the stage of transport:

- leakage of CO_2 from transport pipelines, presenting hazard to humans and animals in the area of the cloud of the released gas,
- risk of exposure to the jet of gas with a very low temperature,
- leakage of CO_2 from the installation and from intermediate storage points.

The most typical factors that cause damage to pipelines are corrosion, defects of the pipeline material, movements of the ground or the action of third parties, especially during earthworks [20].

Health hazard related to the impact of CO_2 on humans and animals concerns the effects of a high concentration of CO_2 on the one hand, and the effects of a decreased concentration of oxygen on the other. In higher concentrations, carbon dioxide has an adverse impact on human behaviour and health. 1% concentration causes drowsiness and the value of 1.5% is the maximum concentration permissible in some professions, for example for submarine crews. Concentrations exceeding 2% have a slightly narcotic effect and result in higher blood pressure and pulse. Carbon dioxide also affects hearing acuity. In concentrations ranging from 3% to 5% it impedes breathing, raises blood pressure significantly, causes dizziness and headaches. It multiplies the heart beat and it may bring about fits of panic. Additionally, at concentrations higher than 10%, loss of consciousness may occur and longer exposure results in suffocation. Concentration exceeding 20% causes immediate death.

4.2. The model of phenomena occurring in a damaged pipeline

Immediately after the pipeline is damaged, the pressure of the condensed carbon dioxide decreases abruptly. The rate of this drop depends on the speed of sound in this liquid and, in the final phase of the process in the pipeline, CO_2 reaches the parameters of a saturated liquid. The course of the process may in fact be complicated significantly by factors such as waves generated in the pipeline or the impact of the elasticity of the pipeline itself. Thermodynamically, this process is not a simple process of isentropic, isenthalpic or isothermal expansion, but experimental measurements show that no substantial changes in temperature occur in it. Considering subsequent phenomena, it is justified to assume that at the end of this process the parameters that correspond to the initial temperature T_0 and the saturation pressure in this temperature $p_0 = p_{sat}$ (T_0) stabilize in the pipeline. Now the process of evaporation starts and a further drop in pressure at the expense of the heat absorbed from the liquid and the pipeline walls occurs. Evaporation begins at the location of the rupture and moves towards the pipeline end (Fig. 9).

This means that in either of the two parts of the pipeline determined by the rupture there exist two zones: the saturated liquid zone (1) with constant temperature T_0 and pressure p_0 and a two-phase zone (2). The content of the gas fraction in zone 2 changes from zero in the "b" cross section separating areas (1) and (2) to one in the outflow zone. The liquid flows towards the

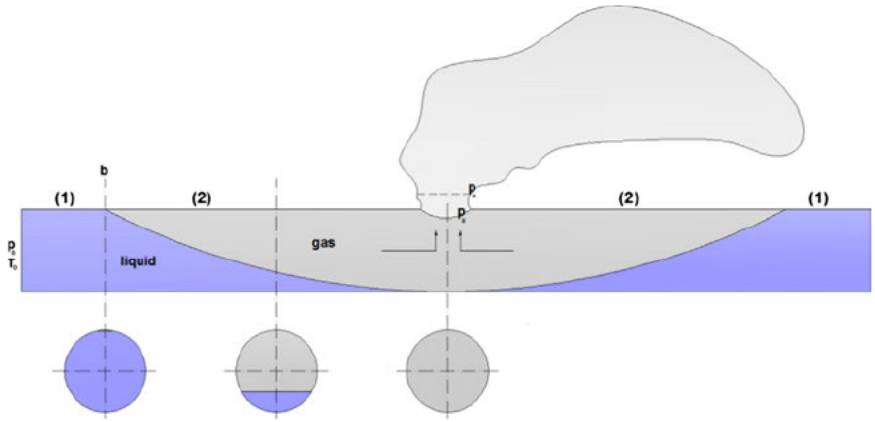

Fig. 9. Outflow of gas from a damaged pipeline.

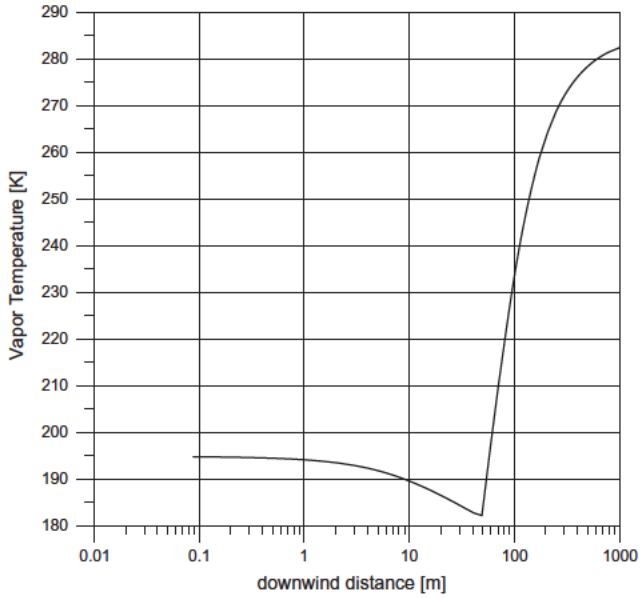

Fig. 10. Drop of CO_2 temperature during the outflow to the surroundings.

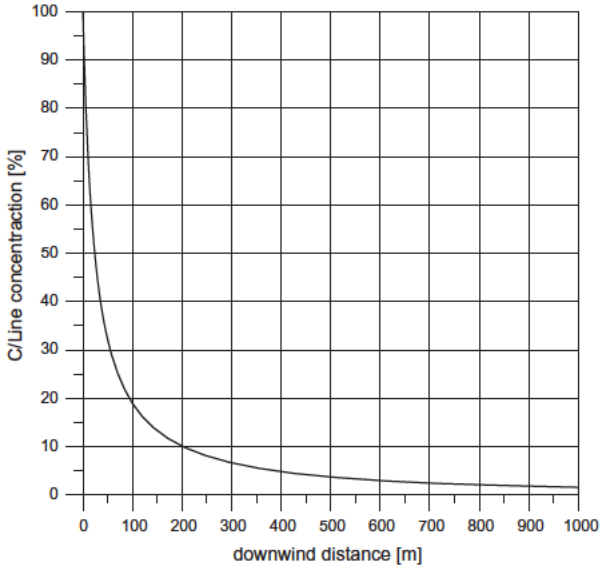

Fig. 11. Change in CO_2 concentration depending on distance.

hole with increasing content of the gas fraction and a simultaneous decrease in pressure to a certain value of p_e at the place of the outflow. The flow speed in zone 2 is therefore a resultant of the drop in pressure and the rate of expansion caused by evaporation.

The outflow of gas through the hole in the pipeline is most of the time a choked one. This causes that atmospheric expansion of carbon dioxide to ambient pressure p_a takes place in the immediate vicinity of the rupture.

Another stage of the propagation of carbon dioxide from the damaged pipeline is its transport in surrounding air. At the beginning, the jet of released gas has a circular cross section which takes the shape of a truncated ellipsis after touching the ground. To describe these phenomena the Unified Dispersion Model (UDM) is used, which assumes that dispersion is composed of three phases: the jet release phase, the heavy gas phase and the passive transport phase [21]. The outflow of the CO_2 jet may be a two-phase one, a further consequence of which may be the fall of droplets, a formation of a pool and its subsequent evaporation. The UDM mathematical model forms a set of differential equations comprising, among others, the mass conservation equation, the momentum conservation equation, the relations describing the speed of the cloud, its location, the heat exchange, the propagation of the cloud in the directions transverse to the wind direction, etc.

4.3. The assessment of the hazard zone around a damaged pipeline

The PHAST software package ver. 6.7 with implemented models of flow phenomena in a damaged pipeline, including the UDM, is used for the calculations. The performed calculations relate to the rupture of a 0.45 m diameter pipeline in which carbon dioxide is transported in the liquid state at the pressure of 152.6 bar. The mass flow of the CO_2 is 156.4 kg/s. Upon rupture, a hole appears in the pipeline with an area corresponding to 20% of the pipeline diameter. As it was mentioned above, carbon dioxide released into the atmosphere gets cooler, and the range of the temperature fall depending on the distance measured in the wind direction is shown in Fig. 10. The gas minimum temperature may reach 90 °C. The change in CO_2 concentration in the central line of the formed cloud depending on distance is shown in Fig. 11. The maximum range of 5%, 10% and 20% CO_2 concentration is shown in Fig. 12. It makes it possible to state that the zone of the 5% concentration of gas reaches as far as 380 m and the zone of 20% concentration extends over a distance of almost 90 m. The time for such concentration to remain depends on the amount of the released gas.

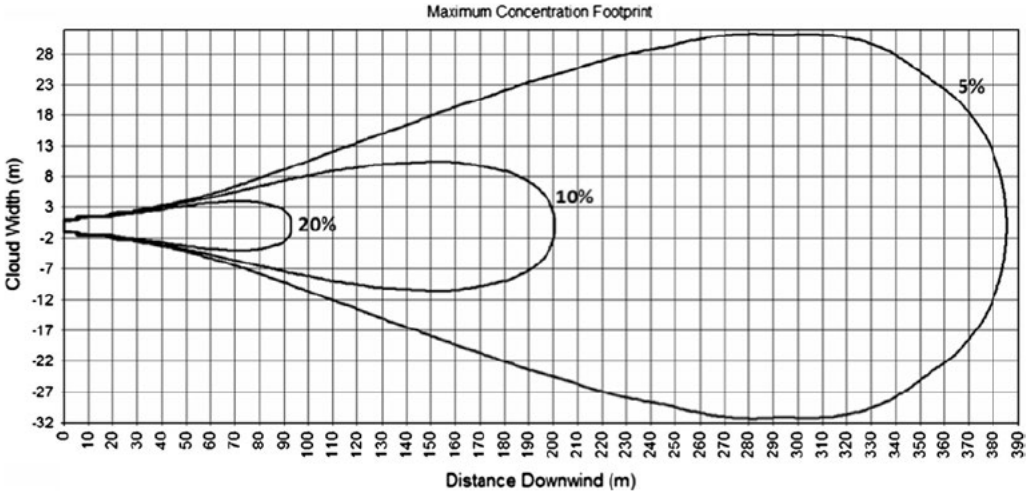

Fig. 12. Areas corresponding to 5%, 10% and 20% concentration of CO_2.

5. Conclusions

Four different feasible strategies for compressing CO_2 in a coal-fired power plant with post-combustion CO_2 capture were studied. Their performance was quantified and compared with a conventional compression solution. This study emphasizes that the total compression power is a strong function of the thermodynamic process and is not only determined by the compressor efficiency. To optimize heat integration, compression systems must be integrated with both the power unit and the CO_2 capture installations. If successful, the two stage shock wave technology with high efficiency and a high pressure ratio [15] is expected to reduce the capital cost of CO_2 compression equipment by as much as 50%, and reduce the operating costs of carbon dioxide capture and sequestration systems by at least 15 percent. An additional benefit is that the stage discharge temperature ranges from 246 °C to 285 °C, depending on the inlet gas and cooling water temperatures. The power required for compression could be reduced if CO_2 was first compressed to an intermediate pressure, then cooled and liquefied, and if that liquid was then pumped to a higher pressure level required for pipeline injection. This paper also studied the effect of such factors as the ambient temperature and the thermal insulation layer on the thermodynamic properties of the CO_2 flow in the pipeline. It proposes certain principles concerning the design of CO_2 transport pipelines and the determination of their safe length without the thermal insulation layer to ensure a minimum pressure drop in the Polish atmospheric conditions. A leak from high pressure pipelines can result in hazard to humans. Therefore, safety considerations require that safety zones should be established around such pipelines, and that the pipelines should be fitted with safety valves that, in the case of rupture, shut off the damaged section of the pipeline, limiting in this way the amount of gas released into the surroundings.

Acknowledgements

The results presented in this paper were obtained from research work co-financed by the National Centre Research and Development in the framework of Contract SP/E/1/67484/10 – Strategic Research Programme – Advanced technologies for energy generation: Development of a technology for highly efficient zero-emission coal-fired power units integrated with CO_2 capture.

References

[1] Singh D, Croiset E, Douglas PL, Douglas MA. Techno-economic study of CO2 capture from an existing coal-fired power plant: MEA scrubbing vs. O_2/CO_2 recycle combustion. Energy Convers Manage 2003;44:3073–91.
[2] Giuffrida A, Matteo C, Lozza R, Lozza G. CO_2 Capture from air-blown gasification-based combined cycle. In: Proceedings of ASME turbo expo; 2012. p. 1–10.
[3] Barker DJ, Turner SA, Napier-Moore PA, Clark M, Davison JE. CO_2 capture in the cement industry. Energy Proc 2009;1:87–94.
[4] Johansson D, Franck PA, Berntsson T. CO_2 capture in oil refineries: assessment of the capture avoidance costs associated with different heat supply options in a future energy market. Energy Convers Manage 2013;66:127–42.
[5] Łukowicz H, Mroncz M. Basic technological concepts of a "capture ready" power plant. Energy fuels. ACS Publications; 2012. p. 6475–6481.
[6] Det Norske Veritas: Design and Operation of CO_2 Pipelines. Recommended, practice, DNV-RP-J202; April 2010.
[7] McCoy ST, Rubin ES. An engineering-economic model of pipeline transport of CO_2 with application to carbon capture and storage. Int J Greenhouse Gas Control 2008;2(2):219–29.
[8] Zhang ZX, Wang GX, Massarotto P, Rudolph V. Optimization of pipeline transport for CO_2 sequestration. Energy Convers Manage 2006;47:702–7115.
[9] Zhang D, Wang Z, Sun J, Zhang L, Zheng L. Economic evaluation of CO_2 pipeline transport in China. Energy Convers Manage 2012;55.
[10] Ramgen Power Systems: Workshop on future large CO_2 Compression systems. Gaithersburg; March 30–31, 2009.
[11] Botero C, Finkenrath M, Belloni C, Bertolo S, D'Ercole M, Gori E, et al. Thermoeconomic evaluation of CO_2 compression strategies for post-combustion CO_2 capture applications. In: Proc. of ASME turbo expo 2009.
[12] Moore JJ, Nored MG. Novel concepts for the compression of large volumes of carbon dioxide. In: Proceedings of ASME turbo expo 2008.
[13] Lawlor S. CO_2 Compression using supersonic shock wave technology. Ramgen power, system; September 15, 2010.
[14] Koopman AA, Bahr DA. The Impact of CO_2 compressor characteristics and integration in post-combustion carbon sequestration. comparative economic analysis. In: Proc. of ASME turbo expo; 2010.
[15] Lupkes K. Ramgen supersonic shock wave compression and shock wave compression and engine technology, 2012 NETL CO_2 capture technology meeting, Pittsburgh, PA; 2012.
[16] Aspen, Version 7.0, User guide; 2008.
[17] Lüdtke KH, editor. Process centrifugal compressors. Berlin (Heidelberg): Springer Verlag; 2004.
[18] Beggs HD, Brill JP. A study of two-phase flow in inclined pipes. J. Petrol. Technol. 1973(May):607–17.
[19] Incropera FP, DeWitt DP. Introduction to heat transfer. 3rd ed. New York: John Wiley & Sons, Inc.; 1996.
[20] Koornneef J, Spruijt M, Molag M, Ramirez A, Turkenburg W, Faaij A. Quantitative risk assessment of CO_2 transport by pipelines – a review of uncertainties and their impacts. J. Hazard. Mater. 2010;177:12–27.
[21] Witlox HWM, Stene J, Harper M, Hennie Nilsen S. Modeling of discharge and atmospheric dispersion for carbon dioxide releases including sensitivity analysis for wide range of scenarios. Energy Proc 2011;4:2253–60.